

Energy approach for earthquake induced slope failure evaluation

Proposition du moyen d'évaluation de l'approche énergétique pour la quantité déformé induite par l'écoulement de la pente en cas de tremblement de terre

T. Ishizawa, T. Kokusho, T. Harada & S.Nemoto

Department of Civil Engineering, Chuo University, Tokyo, Japan

ABSTRACT

Earthquake-induced slope stability has been evaluated by the force-equilibrium of soil mass in normal engineering practice. But this method can't evaluate how large the deformation will develop and how far the effect reaches down-slope in flow-type failures. This study aims the development of evaluation method for flow displacements of slopes during earthquake in terms of energy. An innovative model test is developed, in which the energy dissipated in slope failure is measured on a shake table. Based on the theoretical considerations on the simplified block model and the model tests, a framework of performance based design for slopes against earthquakes has been proposed.

RÉSUMÉ

La stabilité d'un terrain en pente, lors d'une secousse sismique, est généralement évaluée par l'équilibre de force entre les masses de terre. Cependant, cette méthode n'est pas efficace pour permettre les évaluations de la quantité de déformation après destruction et de l'étendue de l'impact en aval du terrain. Afin d'y remédier et pour disposer d'une méthode d'évaluation crédible, il est impératif de développer une méthode d'évaluation rationnelle de la quantité de déplacement de terre, à la suite d'une destruction provenant d'un séisme. Afin d'améliorer la méthode d'évaluation de la stabilité de terrain pentu lors d'une secousse sismique, nous avons présenté la structure de la méthode d'évaluation de la quantité de déplacement d'un terrain en pente, du point de vue énergétique, en développant une méthode d'expérimentation, en modèle réduit, pour démontrer les possibilités de celle-ci et avons étudié les résultats obtenus en les comparant avec ceux de la méthode "Newmark".

1 INTRODUCTION

In this research, an energy approach is proposed to evaluate slope failures including flow failures from their initiation to termination. The basic idea of the energy approach proposed by Kokusho (2003) is shown in Fig. 1. Four energies; earthquake energy contributing to the slope failure E_{EQ} , potential energy by the gravity E_p , energy dissipated in soil due to the slope deformation E_{DP} and kinetic energy E_K of sliding soil mass can be correlated by the following equation;

$$E_{EQ} - \delta E_p = E_{DP} + E_K \quad (1)$$

$$\Delta E_{EQ} - \Delta \delta E_p = \Delta E_{DP} + \Delta E_K \quad (1a)$$

Note that the potential energy change before and after failure δE_p or its increment $\Delta \delta E_p$ in Eq.(1a) is normally negative. If the failure mode and the energy dissipation mechanism in sliding soil mass are known, it becomes possible to evaluate how far the failed soil mass will reach in the down-slope direction.

As a first step of the research, an energy balance in a model of a Newmark-type rigid block resting on an inclined plane is examined. Then, an innovative model test is developed, in which the earthquake energy used for slope failure E_{EQ} can be successfully measured, quantifying the energy balance involved in the failure of the model slope. Based on the research findings, a framework of performance based design for slopes during earthquakes is proposed.

2 ENERGY APPROACH TO NEWMARK METHOD

The Newmark Method (Newmark 1965) or its modifications is a commonly accepted practice in geotechnical earthquake engineering to estimate seismically induced displacement of earth-structures. It is based on the force equilibrium of a sliding soil block. Instead of the force equilibrium, Kokusho et al.(2004a) examined the Newmark Model from the viewpoint of

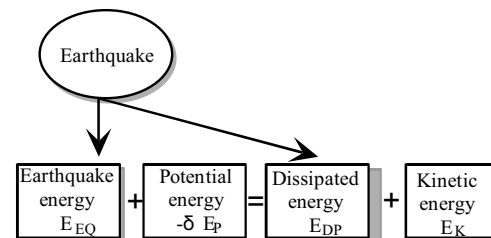


Figure. 1 Energy balance in flow of slope

energy, because the energy concept is more appropriate to evaluate flow displacement. If residual displacement is δ_r , then the potential energy change δE_p is;

$$\delta E_p = -Mg\beta\delta_r \quad (2)$$

where M = the sliding soil mass, g =the acceleration of gravity and β = the slope gradient. The dissipated energy E_{DP} which occurs exclusively along the slip plane in the rigid block model is expressed as;

$$E_{DP} = \frac{\mu(1+\beta^2)}{1+\mu\beta} Mg\delta_r \quad (3)$$

where $\mu = \tan \phi'$ is the friction coefficient between the slope and the block, and ϕ' is the internal friction angle in terms of effective stress. From Eq.(1), the earthquake energy contributing to the block slippage is;

$$E_{EQ} = \delta E_p + E_{DP} = \frac{\mu - \beta}{1 + \mu\beta} Mg\delta_r \quad (4)$$

and the kinetic energy E_k is zero if the energies after the complete stop of slope failure is concerned.

Hence, the ratios of E_{EQ} to E_{DP} and E_{EQ} to $-\delta E_p$ are;

$$\frac{E_{EQ}}{E_{DP}} = \frac{\mu - \beta}{\mu(1 + \beta^2)}$$

$$\frac{E_{EQ}}{-\delta E_p} = \frac{\mu - \beta}{\beta(1 + \mu\beta)}$$

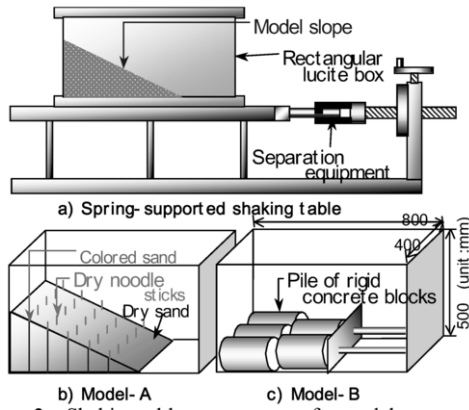


Figure.2 Shaking table test apparatus for model slopes (Model-A versus Model-B).

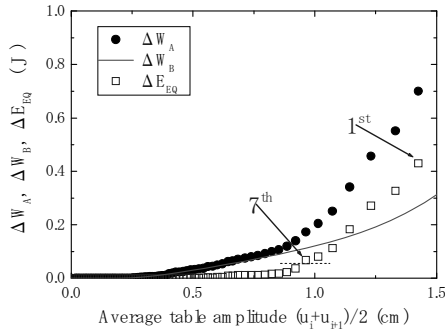


Figure.4 Dissipated energy obtained as a difference of loss energies in Model-A and B.

The ratios are totally independent of seismic coefficient k and depends only on slope inclination β and friction coefficient μ (Kokusho et al. 2004).

3 SHAKE TABLE MODEL TESTS

A model consisting of dry sand is tested on a shake table to quantify energies involved in the slope failure more realistic than the Newmark-type model. A spring-supported shaking table shown in Fig.2 was utilized to apply vibrations to a model slope made from sand, called Model-A here, in a rectangular lucite box. The model slope was made by air-pluviating dry clean Toyoura sand to a total soil mass 30kg to a prescribed relative density of $Dr \approx 40\%$. The slope angle was 29 degrees ($\beta = \tan 29^\circ = 0.55$). In order to evaluate the friction coefficient μ of the model slope, the slope was gradually inclined statically until the onset of slope failure. The static tests carried out four times with the same initial slope angle of 29 degrees and $Dr \approx 40\%$ gave the angle of repose 35.1° to 36.0° (average 35.4° , $\mu = \tan 35.4^\circ = 0.70$).

The table was initially pulled by a given horizontal displacement and released to generate free vibrations. The dissipated energy which can be calculated from the decay vibration in each cycle depends not only on the energy dissipation due to slope deformation but also on other energy loss mechanisms such as radiation damping in the shake table foundation. In order to evaluate the dissipated energy due to slope deformation, a dummy model, called Model-B here consisting of a pile of rigid concrete blocks, was made in the same lucite box and vibrated in the same way as shown in Fig.2. The total mass and the center of gravity were adjusted to be

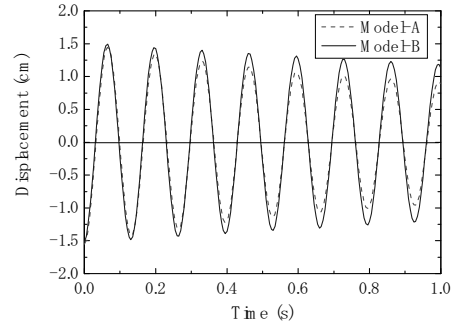


Figure. 3 Decay vibrations measured by a LVDT displacement gauge in Model-A and B.

almost identical in the two models.

In Fig.3, the decay vibrations measured by a LVDT displacement gauge in the Model-A and B are shown. Note that, though the initial table displacement $u_0 = 1.5$ cm are almost the same, the difference in the amplitudes of the decayed vibration grows larger with increasing number of cycles. It may be reasonable to assume that this difference reflects the energy dissipated in Model-A due to its deformations considering that almost negligible energy is dissipative in the rigid concrete blocks in Model-B.

Here, the loss energy per each cycle can be calculated as

$$\Delta W = 4\pi WD = 4\pi \left\{ \frac{1}{2} k \left(\frac{u_i + u_{i+1}}{2} \right)^2 \right\} \left\{ \frac{1}{2\pi} \ln \frac{u_i}{u_{i+1}} \right\} \quad (6)$$

in which W representing the strain energy in the same cycle can be evaluated from the spring constant k , and D representing the damping ratio can be evaluated from u_i and u_{i+1} , displacement amplitudes of the i 'th cycle and $(i+1)$ 'th cycle in the decay vibration, respectively.

The earthquake energy increment in the model slope ΔE_{EQ} can then be evaluated from the loss energies per cycle in Model-A and Model-B, ΔW_A and ΔW_B , respectively as;

$$\Delta E_{EQ} = \Delta W_A - \Delta W_B \quad (7)$$

In Fig.4, ΔW_A evaluated in one of the tests on Model-A is compared with the average curve of the loss energy of Model-B, ΔW_B , evaluated in four tests of the same test condition. ΔE_{EQ} calculated by Eq.(7) for each cycle is also plotted on the same chart indicating that ΔE_{EQ} reduces to almost zero after around 8th cycle. This is consistent with the experimental observation that the residual deformation of the model slope was visible only within first 7 cycles.

The total earthquake energy E_{EQ} calculated as a sum of ΔE_{EQ} in each cycle represents the amount of earthquake energy involved in producing the final displacement in the model slope. To be more precise, E_{EQ} also includes the energy dissipated by soil damping in the model during vibration, which is neglected in the interpretation of the model test results.

4 SLOPE DEFORMATION VERSUS ENERGY

The cycle-by-cycle deformation of the model slope was observed by two video cameras from side and above. Column-shaped markers made from colored sand were installed at the side of the model. On the slope face, dry noodle sticks were set up in line. The interval of these markers was 10 cm in the slope direction. The slope deformation was also measured by a laser beam displacement sensor before and after the test.

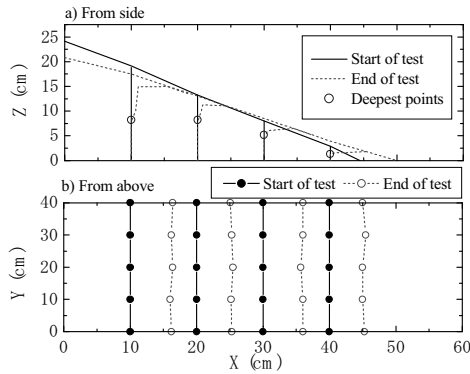


Figure.5 Movement of markers from side at the surface from above.

In Fig.5 movements of markers from side and at the slope surface from above from the start to the end of the test are shown. The plan view of the movement of markers on the slope surface shows that the deformation may be approximated to be uniform in the direction normal to the cross-section. In order to correlate the energies with the residual displacement of the slope, the horizontal residual displacement δ_r was evaluated as an average of the spatially variable measured displacements. To explain more in detail, δ_r was calculated as the average of averaged horizontal displacements along all vertical markers above the deepest points where the deformation was observed as shown in Fig.5. The uniformity of the slope displacement was assumed in the direction normal to the cross-section. This calculation was implemented in each cycle of the input vibration to obtain the incremental residual displacement $\Delta \delta_r$. The potential energy $-\Delta \delta E_p$ is calculated cycle by cycle N from the change of the slope surface configuration as;

$$\Delta \delta E_p = \Delta (\rho_d g B \int z dx dz) \quad (8)$$

where z is the vertical coordinate, ρ_d is the dry soil density and assumed constant. The integration is carried out over the cross-sectional area of the slope. It may be assumed here that the kinetic energy ΔE_K in Eq.(1') is small and ignorable because the velocity of displaced soil mass is not large in this test. Hence,

$$\Delta E_{DP} = \Delta E_{EQ} - \Delta \delta E_p \quad (9)$$

The incremental energies, ΔE_{EQ} , $-\Delta \delta E_p$ and ΔE_{DP} calculated in each cycle are summed up from the first to 7th cycle to evaluate corresponding total energies, E_{EQ} , $-\delta E_p$ and E_{DP} . In Fig.6, the values of $-\delta E_p$ and E_{DP} in the vertical axis are plotted versus the earthquake energy E_{EQ} in the horizontal axis for several test cases with different initial table displacement. According to the solid line approximating the plots of $-\delta E_p$ versus E_{EQ} , it is obvious that the potential energy change $-\delta E_p$ contributes about three times more to the slope failure than the earthquake energy E_{EQ} due to relatively large slope angle, although the latter serves as a trigger of slope failure.

In the light of the energy ratios for the Newmark Model, E_{DP}/E_{EQ} and $-\delta E_p/E_{EQ}$ can be calculated theoretically by Eq.(5) based on the rigid block model. Because the angle of the slope is 29 degrees ($\beta=0.55$) and the angle of repose of the sand is about 35 degrees ($\mu=0.70$), $E_{DP}/E_{EQ}=6.1$ and $-\delta E_p/E_{EQ}=5.1$. These two relations are drawn in Fig.6 by two dashed lines. Obviously there is a wide gap between the theory on the rigid body model and the sand slope. However, the experimental results may also be roughly approximated by straight lines, indicating that $-\delta E_p$ and E_{DP} tend to increase almost in proportion with E_{EQ} irrespective of the intensity of shaking. This further indicates that the energy formulations on

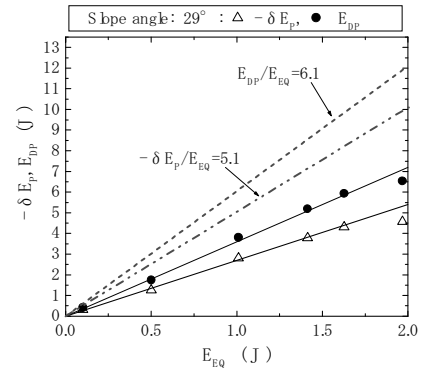


Figure.6 Earthquake energy E_{EQ} versus potential energy $-\delta E_p$ or dissipated energy E_{DP} .

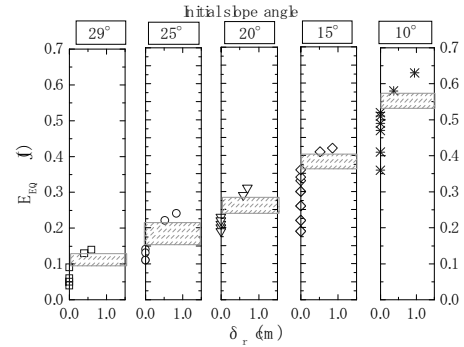


Figure.7 Relationship between residual displacement δ_r and earthquake energy E_{EQ} with different the initial slope angle.

the rigid block model can capture an important part of the slope failure mechanism and be applicable to a deformable soil slope with a modification of the friction coefficient μ .

5 THRESHOLD ENERGY FOR INITIATING SLOPE DEFORMATION

In order for a threshold value in the earthquake energy E_{EQ} for initiating the slope failure, the initial table displacement u_0 was gradually increased until initiating the slope failure. The relative density was kept constant ($Dr \approx 40\%$) and the initial angle of the slope was parametrically changed from 10 degrees to 29 degrees (the slope inclination $\beta: 0.18 \sim 0.55$).

In Fig.7, the earthquake energy E_{EQ} is plotted versus the residual displacement δ_r at the end of shaking obtained by several tests with different initial slope angle. Threshold energies are clearly recognized as shaded zones separating occurrence or nonoccurrence of residual slope deformation. The thresholds become smaller with larger initial slope angles. Hence, it is conceivable that an initiation of residual slope deformation can also be evaluated by the earthquake energy E_{EQ} in place of acceleration or seismic coefficient.

6 PERFORMANCE BASED SLOPE EVALUATION BY ENERGY APPROACH

Based on the theoretical considerations on the simplified block model and the model tests explained above, a framework of a performance based design for earthquake-induced slope failures by the energy approach may be proposed as shown in Fig.8.

First, the input earthquake energy E_{IP} defined at the base of slopes or embankments for evaluating stability is designated site by site. How to evaluate the input energy is available in another literature (Kokusho et al.2004b).

By assuming the energy E_{rd} by radiation damping at the base, the earthquake energy E_{EQ} to be consumed inside the slopes or embankments can be given. In the model test, the total input energy applied to the shaking table E_{IP} can be calculated from the initial pull displacement of the table and a almost constant ratio $E_{EQ}/E_{IP} \approx 0.25$ has been found irrespective of the extent of slope failure (Kokusho et al 2004). In practical problems, the ratio may be evaluated by conducting a 1-D multi-reflection analysis of the SH-wave (Kokusho.2004b) on a simplified model including a sloping ground and its base layer.

The energy $(E_{IP} - E_{rd})$ is dissipated by residual slope deformation and by internal soil damping. It may not be so difficult to estimate the energy associated E_{EQ}' with internal soil damping based on FEM analyses of slopes. This energy E_{EQ}' is somehow related with the threshold energy previously discussed above which slope failure starts. Hence, the earthquake energy to be used for the residual slope deformation E_{EQ} can be differentiated as;

$$E_{EQ} = E_{IP} - E_{rd} - E_{EQ}' \quad (10)$$

Based on the Newmark-type simple model, the residual horizontal displacement is expressed based on Eq.(4) as;

$$\delta_r = \frac{(1 + \mu\beta) E_{EQ}}{(\mu - \beta) Mg} \quad (11)$$

The thickness or the mass of sliding soil M may be determined by conventional slip surface analyses.

Incidentally, in Fig.9, the residual displacements δ_r at the end of shaking obtained by several tests with different initial table displacements are plotted versus the normalized earthquake energies E_{EQ}/Mg . The weight of the displaced soil mass M is evaluated from the soil mass above the deepest points in Fig.5. Despite the data scatters, the test results may be approximated by a dotted straight line passing through the origin. On the other hand, the theoretical line by Eq.(11) for $\beta = 0.55$ and $\mu = 0.70$ is drawn in Fig.9 by the solid line. Despite the clear difference in the inclination between the two lines, it may be said that the solid block model captures the basic features of failure mechanism of the soil slope.

Whenever there was severe damage by seismically induced slope failures, soil strength seems to have drastically decreased due to pore pressure buildup or some other reasons. In this test, too, if saturated sand were used in place of dry sand, the slope may have experienced larger flow-type displacement. In order to take such a failure modes into considerations, the coefficient $(1 + \mu\beta)/(\mu - \beta)$ in Eq.(11) may be modified in accordance with model test results or case studies of previous slope failures.

These are the essence of the slope evaluation procedures by the energy approach. Much more work by model tests, case history studies, etc. is needed to establish reliable evaluation methods.

7 CONCLUSIONS

The energy approach has been applied to slope failure evaluation first by examining the energy balance in the Newmark-type block model and then by carrying out an innovative shake table tests of a model slope of dry sand, yielding the following major findings.

1. The energy balance in the Newmark-type model indicates that the ratio of the earthquake energy used for slope failure E_{EQ} to the potential energy $-dE_p$ or the energy dissipated in the slope E_{DP} is independent of seismic coefficient k and depends only on slope gradient β and friction coefficient μ .
2. The earthquake energy used for slope failure E_{EQ} can be successfully measured in the innovative model test developed in this research, quantifying the energy balance

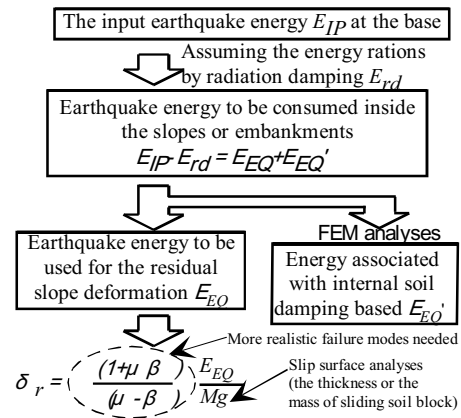


Figure.8 Performance based slope evaluation by energy approach.

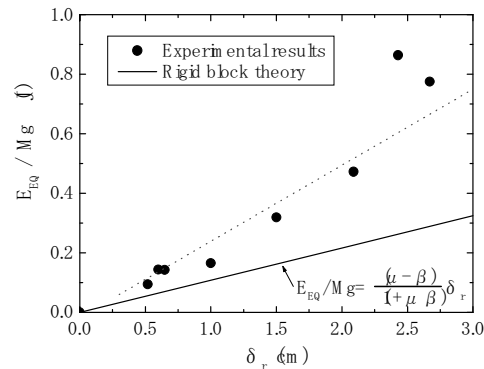


Figure.9 Relationships between residual displacement δ_r and earthquake energy E_{EQ} .

involved in the failure of the model slope.

3. The residual displacement δ_r versus normalized earthquake energy E_{EQ}/Mg relationship derived here is somewhat different between the rigid block model and sand slopes reflecting the difference of failure mechanism between the two models.
4. It is conceivable that a threshold value for occurrence of nonoccurrence of residual slope deformation can be evaluated by the Earthquake energy E_{EQ} . The threshold value becomes smaller with larger initial slope angle, and the earthquake energy for initiating the slope failure becomes smaller with larger initial slope angle.
5. Based on the above results, a framework of the energy approach for evaluating slope deformation in practical designs has been proposed. In order to upgrade this to a reliable design tool, more research on the energy balance in complex in situ conditions is needed.

REFERENCES

- T. Kokusho and K. Kabasawa, "Energy approach to flow failure and its application to flow due to water film in liquefied deposits," Proc. of International Conference on Fast Slope Movement, Naples, May 2003.
- N. M. Newmark, "Effects of earthquakes on dams and embankments," Fifth Rankine Lecture, Geotechnique Vol.15, pp.139-159, 1965.
- T. Kokusho, T.Ishizawa and T.Harada, "Energy approach for earthquake induced slope failure evaluation" Proc.11th International Conference on Soil Dynamics & Earthquake Engineering and 3rd International Conference on Earthquake Geotechnical Engineering, Berkeley, California, Vol.2,260-267,2004a.
- T. Kokusho, R.Motoyama, S.Mantani and H.Motoyama "Seismic wave energy evaluation in surface layers for performance-based design". Prof. of 13WCEE, Vancouver, Paper, California, No.3480, 2004b.